

EXPERIMENTAL STUDY OF THE ACOUSTIC SPINNING MODES
GENERATED BY A HELICOPTER TURBOSHAFT ENGINE

S. Léwy and H. Gounet

Office National d'Etudes et de Recherches Aérospatiales (ONERA),

BP 72, 92322 Châtillon, France

Abstract

Turboshaft engines may be the main noise source radiated by helicopters during take-off, if the sound levels are measured in dBA or PNdB. The engine inlet is often non-axisymmetric and one can take advantage of this for reducing the ground perceived noise simply by modifying the radiated directivity. The study is focused on the blade passing frequency of the first axial compressor, which dominates the acoustic spectra. The objective is to better understand the space structure (spinning modes) of the generated waves in order to predict the directivity pattern (model of Tyler and Sofrin). The tests were performed at the Turbomeca outdoor facility. Some experiments using an array of fixed microphones in an inlet cross section of a TM333 engine show that the spinning mode analysis can yield useful results even if the cross section is far from being circular. However, the number of microphones remains necessarily small, which entails a spatial aliasing on high-order modes. Tests were thus conducted with moving microphones in the very near field of an Arriel engine, just outside the intake. The measured spinning modes can be used as input data into a computer code predicting the far field directivity.

Nomenclature

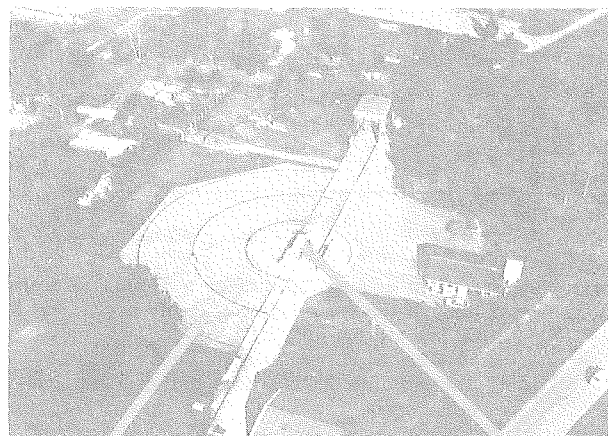
- a : Celerity of sound
- A_m : Modal component at a given frequency
- B : Number of rotor blades
- d : Distance of spinning-mode measurement outside the engine intake
- f : Frequency
- f_c : Cut-off frequency of an acoustic mode
- H, L : Lengths of a rectangular duct cross section
- J_m : Bessel function of the first kind, of order m
- K : Total wave-number ($= 2 \pi f/a$)
- k : Axial wave-number
- k_T, k_x, k_y : Transverse wave-numbers
- l, n : Acoustic mode order in a rectangular duct
- M : Mean flow Mach number inside the duct
- m, μ : Acoustic mode order in a cylindrical duct
- N : Compressor rotational speed
- p : Sound pressure
- P_o : Complex multiplicative constant in the sound pressure expression
- R : Duct radius
- r, θ, z : Cylindrical coordinates in the duct
- S : Cross spectrum
- t : Time
- V : Number of stator vanes
- x, y, z : Cartesian coordinates in the duct
- Δf : Frequency bandwidth
- ξ : Cut-on ratio of an acoustic mode ($= f_c/f$)
- φ : Angle of the radiated sound directivity
- $X_{m\mu}$: Abscissa of the $(\mu + 1)$ th extremum of J_m
- ω : Angular frequency ($= 2 \pi f$)

Abbreviation

BPF : Blade passage frequency (= BN)

I. Introduction

Turboshaft engines may be the main noise source radiated by helicopters during take-off, if the sound levels are weighted to represent the nuisance due to the aircraft (for instance A-weighted levels, in dBA, or Perceived Noise levels, in PNdB).^(1,2) Tests have been performed for several years at the Turbomeca outdoor facility located near Pau in the South of France (Fig. 1).⁽³⁾ Conventional far-field directivities are of prime importance to build up semi-empirical acoustic computations, which predict for instance the contribution of the engines to total aircraft noise under various flight conditions. Information however is still scarce for research purpose. The most useful parameter is the space (or modal) structure at each frequency of the acoustic field propagating in the intake or in the nozzle. The present study is focused on the blade passing frequency (BPF) of the first axial compressor stage, which dominates the acoustic spectra, mainly in the upstream arc (Fig. 2, from Ref. 4).



Semi-circular concrete ground (microphone rails at 10 m, 20 m and 30 m) Engine height : 3 m

Figure 1 - General view of the Turbomeca outdoor test facility.

- The three main applications may be the following ones.
- 1) Effective noise reduction requires a better understanding of the acoustic sources. Modal analysis is particularly interesting for the tones emitted by compressors or turbines because the angular symmetries of the rotors and stators determine which spinning modes may be generated. The measured mode levels indicate which mechanisms produce the strongest sources (for instance waves due to transonic rotors or interactions between successive rows).
 - 2) Optimization of acoustic linings on the inlet duct requires the wave incidence angle on the wall, which is determined by the modal structure.
 - 3) The simplest way of predicting directivity is to use the Tyler and Sofrin model.⁽⁵⁾ The input data are the modal contents of

the sound field in the exit section of the duct.⁽⁶⁾ The duct introduces some cut-off properties, and only the lower generated modes can propagate and radiate into the free field.

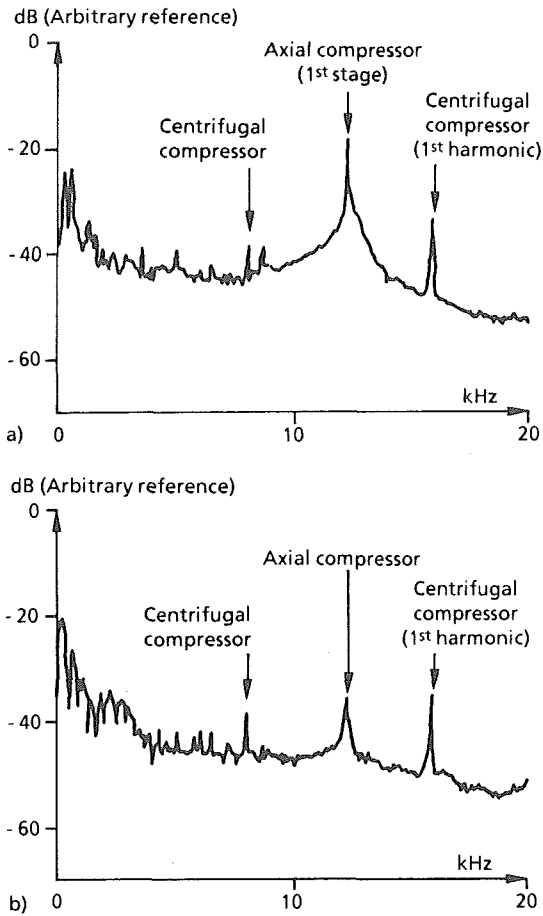


Figure 2 - Far-field acoustic spectra of a TM333 turboshaft engine at the twin-engine take-off power: 465 kW (623 SHP). From Ref. 4.
 . $\theta = 0$ on the upstream engine center line
 . The dB reference is arbitrary, and is the same for both curves.

- a) Upstream radiation: $\theta = 40$ deg.
- b) Downstream radiation: $\theta = 130$ deg.

The third item is the most important at the present time because the intake is often non-axisymmetric and one can take advantage of this for reducing the ground perceived noise simply by modifying the directivity pattern. The theory of Refs. 5 and 6 is very well known and validated for simple geometries (straight ducts of circular, annular or rectangular cross sections). Although some extensions were published for transmission through curved duct bends of constant section,^(7,8,9) the intake geometry of a turboshaft engine is generally too complex to develop a satisfactory model. This article thus presents some experimental results on the duct transfer function between the acoustic sources and the exit plane, based on spinning mode analysis. Two methods are used. Section 2 presents the theoretical background and test results obtained using an array of fixed microphones flush mounted on the duct wall in the non-axisymmetric inlet of a TM333 engine. Section 3 shows that similar information may be deduced from measurements with moving microphones on a ring located just in front of the intake, in the case of an axisymmetric Arriel engine.

II. Spinning Mode Analysis in the Intake Duct with Fixed Microphones

The tests were performed with a TM333 turboshaft engine at the Turbomeca outdoor facility (Fig. 1). The engine centerline is at a height of 3 m. The engine is loaded by a hydraulic brake (Fig. 3a) which absorbs the shaft power up to about 1700 kW or 2300 SHP (this covers all the engine ratings corresponding to the various aircraft flight conditions). The spinning-mode spectra in a duct cross section can be measured using an array of fixed, equidistant, flush-mounted microphones.⁽¹⁰⁾ Special data processing had to be developed for the present application because of the low signal to noise ratio due mainly to the highly turbulent flow over the microphone grids. Some results were already published for measurements inside the TM333 nozzle.⁽¹¹⁾ The problem is far more complicated in the case of the intake because of its complex cross section. The noise is mainly generated by the first compressor stage which is of course enclosed in a circular duct, but the inlet tends to become more "rectangular" farther upstream (Fig. 3b) where modal analysis is required for predicting the free-field directivity.

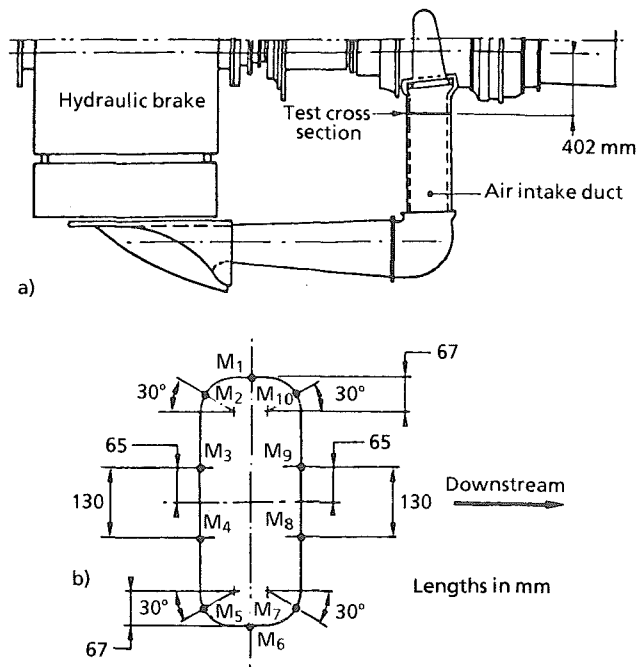


Figure 3 - Acoustic mode measurement in the inlet of a TM333 turboshaft engine.
 a) Upper view of the engine in the Turbomeca test bench
 b) Location of the microphones (M_1 to M_{10}) in the test cross section.

Theoretical Background

The spinning-mode reduction is related to the eigenfunctions of the wave equation in cylindrical coordinates, and thus applies to ducts with circular or annular cross sections. The equivalent solution in cartesian coordinates for rectangular ducts gives transverse standing modes, which are quite different. A mode is defined by the frequency $f = \omega / (2\pi)$ and two integers:

- m and μ in cylindrical coordinates (r, θ, z) , where m is the angular wave-number and μ is the radial mode;
- l and n in rectangular coordinates (x, y, z) where l and n are the orders of the transverse wave-numbers, respectively in the x and y directions (z is the duct axis).

The main characteristics of the ducted propagation are given by the cut-off properties of guided waves. They are based on the

dispersion relationship:

$$(K - Mk)^2 = k^2 + k_T^2 \quad (1)$$

where $K = 2\pi f/a$ is the total wave-number (a is the celerity of sound), k is the axial wave-number, k_T the transverse wave-number, and M is the mean flow Mach number inside the duct. A mode may propagate if k is real, or:

$$K \geq \sqrt{1 - M^2} \cdot k_T, \text{ or} \quad (2)$$

$$f \geq f_c \text{ with } f_c = \sqrt{1 - M^2} \cdot ak_T / (2\pi)$$

i.e. if its frequency f is greater than the cut-off frequency f_c . It can be noted that the value of M is of little importance in low

subsonic flows since $\sqrt{1 - M^2} \approx 1$.

The transverse wave-number k_T is determined by the boundary conditions at the duct wall, and by the 2π angular periodicity in cylindrical coordinates, which entail only discrete values for k_T , referred to the two integers m and μ , or l and n . Let us consider a rigid-wall duct. If its cross section is circular, of radius R , we have:

$$k_T = \chi_{m\mu} / R, \text{ or } f_c(m, \mu) = \sqrt{1 - M^2} \cdot a \chi_{m\mu} / (2\pi R) \quad (3)$$

where $\chi_{m\mu}$ is the abscissa of the $(\mu + 1)$ extremum of the Bessel function J_m of first kind and of order m . The cut-off frequency increases with μ . Since the symmetries of rotor and stator only produce selection rules on the m values, a mode m can propagate if the frequency f is greater than the cut-off frequency of the first radial mode, $\mu = 0$, i.e.:

$$f_c(m) \equiv f_c(m, \mu = 0) \quad (4)$$

One should also notice that m can be positive or negative, which means that the helical waves are co-rotating or contra-rotating as compared with the source rotation. This distinction is very important to identify the noise sources since $+m$ and $-m$ are due to different rotor loading harmonics. However, $+m$ and $-m$ have the same cut-off frequency and the same free-field directivity pattern. The above equations could thus be written with $|m|$ instead of m . Finally the acoustic pressure of a propagative wave inside the duct is given by:

$$p_{m\mu}(r, \theta, z, t) = P_o \cdot J_m(\chi_{m\mu} \cdot r/R) \cdot \exp[i(\omega t - m\theta - kz)] \quad (5)$$

where P_o is a complex constant, and k is deduced from $k_T = \chi_{m\mu}/R$ by Eq. (1).

If the cross section of the rigid-wall duct is rectangular, with lengths L and H in the x and y directions respectively, then:

$$k_T^2 = k_x^2 + k_y^2, \text{ with } k_x = \pi l/L, k_y = \pi n/H \quad (6)$$

and

$$f_c(l, n) = \sqrt{1 - M^2} \cdot \frac{a}{2} \sqrt{\left(\frac{l}{L}\right)^2 + \left(\frac{n}{H}\right)^2} \quad (7)$$

The acoustic pressure of a propagative wave inside the duct is:

$$P_{ln}(x, y, z, t) = P_o \cdot \cos(\pi lx/L) \cdot \cos(\pi ny/H) \cdot \exp[i(\omega t - kz)] \quad (8)$$

(in this formula, the origin $x = y = 0$ is in a corner of a rectangular cross section).

Data Processing

The question thus arises as to whether spinning mode analysis inside the intake can yield useful results or not. The tests are made with ten flush mounted microphones M_1 to M_{10} (Fig. 3b). The data processing and the full equations are detailed in Ref. 11. It suffices for the following discussion to briefly summarize the principle of the procedure. It is based on the cross spectra S_{ij} between the signals of two transducers i and j , located at the same r and z , and at θ_i and θ_j in cylindrical geometry. After a time Fourier transform, the cross-spectrum components at a frequency f are:

$$S_{ij} = \sum_{m, \mu} p_{m\mu}(\theta_i) \cdot p_{m\mu}^*(\theta_j) = \sum_m A_m(r) \cdot \exp [im(\theta_j - \theta_i)] \quad (9)$$

The complex amplitudes A_m depend on r , which is fixed, and the phases are function of the angles θ . If we take for instance $i = 1$ (microphone M_1 in Fig. 3b), an angular Fourier transform of the set of data S_{1j} leads to the spinning-mode spectrum at f , i.e. $|A_m|$ versus m . This very short description shows that the data reduction is a priori not valid in a rectangular duct. The scope of the study is to check the information which can be deduced in the case of Figure 3.

Before any comments on the results, one should be aware of the spatial aliasing which may appear if high-order modes $|m|$ are present in the acoustic field (Nyquist's theorem). More precisely, with 10 microphones, only 10 different values of m can be discriminate, i.e. $-5 \leq m \leq +4$. This means for instance that $m = 8$ would be merged in $m = 8 - 10 = -2$. The maximum frequency at which no spatial aliasing appears can be estimated from Eqs (3) or (7). Let us take:

$a = 340$ m/s, $M \approx 0.3$, $L \approx 0.2$ m and $H \approx 0.5$ m, or $R \approx 0.2$ m (such that the areas LH and πR^2 are of the same order).

Table 1 shows the cut-off frequencies in a circular and in a rectangular duct. The first two lines, $f_c(m) \equiv f_c(m, \mu = 0)$ and $f_c(l = 0, n)$, are also plotted up to higher frequencies in Fig. 4. Any aliasing problem is avoided if $f \leq f_c(m = 5) = 1656$ Hz. Above this value, $m = +5$ is merged in $m = -5$, and above $f_c(m = 6) = 1936$ Hz, $m = \pm 6$ is mixed with $m = \mp 4$.

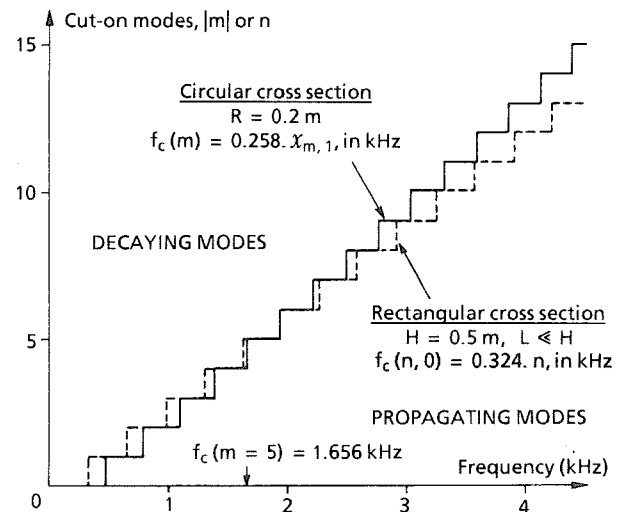


Figure 4 - Theoretical cut-off frequencies in the intake of the TM333 turboshaft engine (flow Mach number $M = 0.3$).

The cut-off frequencies in a circular duct are $f_c(m) = \sqrt{1 - M^2} \cdot a \chi_{m,0} / (2\pi R)$. Figure 4 shows that they

are close to $f_c(l = 0, n) = \sqrt{1 - M^2} \cdot \pi n / (2H)$, if $n = m$ (on the large side H), because it is assumed that $H \approx \pi R$ and because $\chi_{m,0} \approx |m| + 0.81 |m|^{1/2} + \dots \approx |m|$. We can therefore expect that spinning mode analysis can give us a good idea on the propagating waves.

Table I
Cut-off frequencies in circular and rectangular ducts simulating the TM333 intake.
 $a = 340$ m/s, $M = 0.3$, $R = 0.2$ m (upper lines),
or $L = 0.2$ m and $H = 0.5$ m (lower lines).

μ or l \ m or n	0	1	2	3	4	5	6
0	0	475	788	1084	1372	1656	1936
	0	324	649	973	1297	1622	1946
1	989	1376	1731	2069	2393	2715	3029
	811	873	1038	1267	1530	1813	2108
2	1811	2203	2573	2928	3273	$f_c(m, \mu)$ in Hz $f_c(l, n)$	
	1622	1654	1747	2077	2077		

Test Results

Let us consider a test on the TM333 turboshaft engine at the twin-engine take-off power of 448 kW (600 SHP). The signals are analyzed on 15 kHz in 128 bands (frequency resolution $\Delta f = 118$ Hz).

Figure 5 presents the spinning-mode spectra at several frequencies (the central frequency is indicated for each curve) in

the range where there is no spatial aliasing. Some modes exceed the background level by more than 10 dB. They are in good agreement with the predictions in the lines " μ or $l = 0$ " of Table I. At very low frequency, only the plane wave (0,0) may propagate. $|m|$ (or n) = 1 also becomes propagative in the modal spectrum at 413 Hz. $|m|$ (or n) = 2 appears at 767 Hz, and $|m|$ (or n) = 3 at 1121 Hz. These results demonstrate the contribution of a spinning mode analysis even if the duct cross section is far from being circular.

The blade passing frequency raises many more difficulties owing to its very high value:

$$f = BN \approx 12.2 \text{ kHz}$$

(rotor with $B = 17$ blades, rotation speed $N = 43067$ rpm).

According to Eqs (3) and (4), modes $|m|$ up to 44 may then propagate. Figure 6 shows the result in the band centered on 12331 Hz. A special data processing is used here, which removes the modes caused by the background measurement noise thanks to a threshold technique.⁽¹²⁾ We find that:

$$m' = -5, -3, -2, 0, 1, 2 \text{ and } 4,$$

and the actual modes are: $m = m'$ modulo 10. The comments are rendered somewhat confusing by the very large number of possible propagating modes.

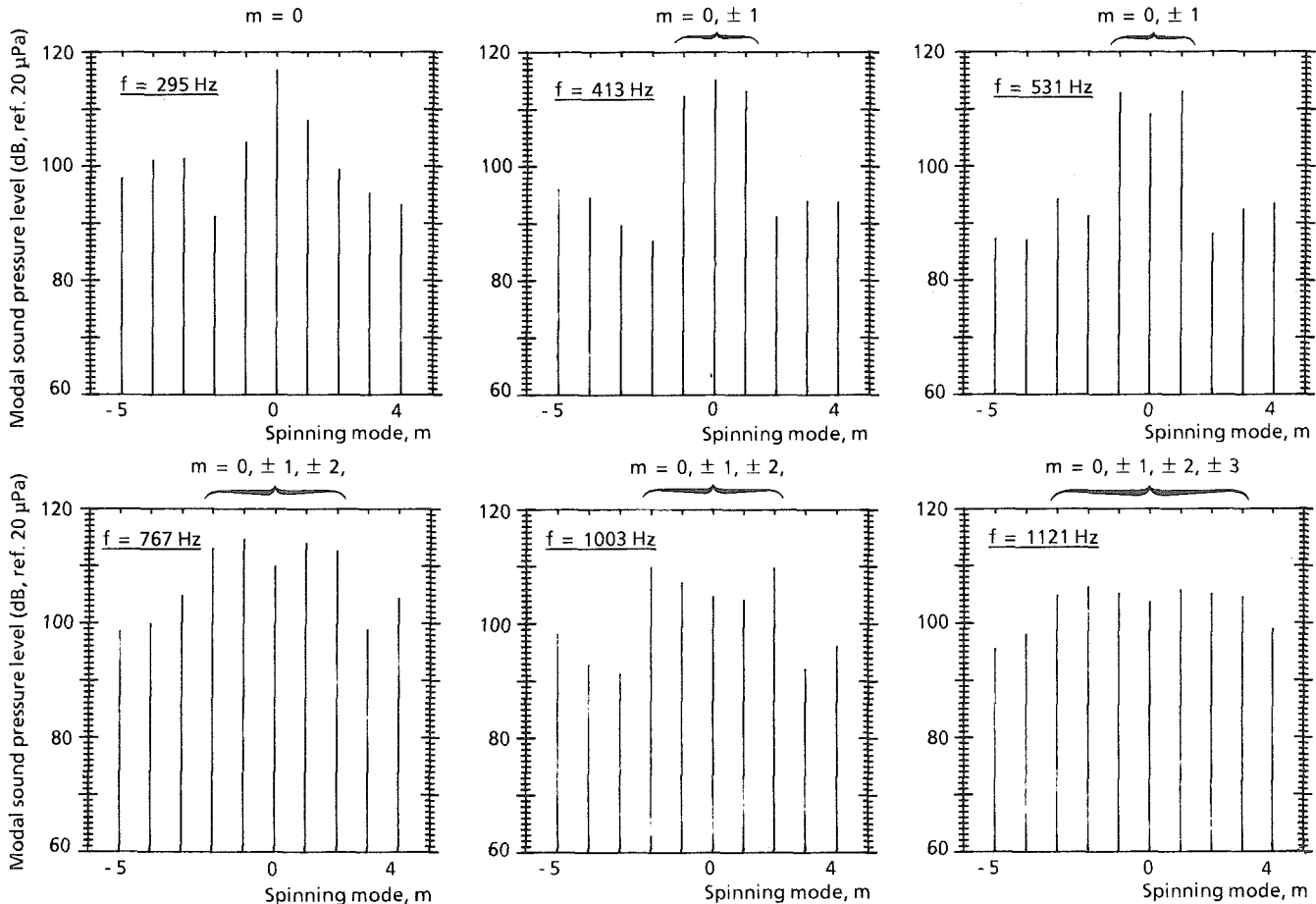


Figure 5 - Spinning-mode spectra at several frequencies (bandwidth $\Delta f = 118$ Hz) in the intake of a TM333 turboshaft engine at the twin-engine take-off power: 448 kW (600 SHP). Measurements with an array of 10 flush-mounted microphones.

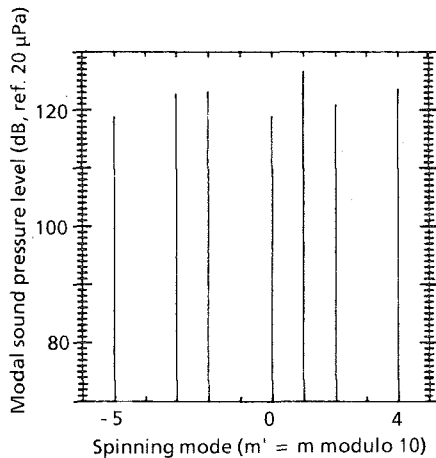


Figure 6 - Spinning-mode spectrum at the blade passing frequency of the TM333 first axial compressor: $f = 12331$ Hz. Same conditions as in the previous figure.

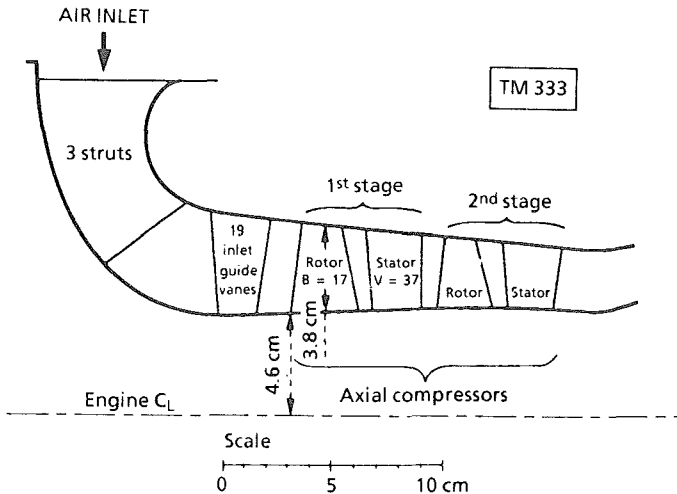


Figure 7 - Diagram of the axial compressor rows in the TM333 turboshaft engine (from a Turbomeca document).

However, the diagram of the TM333 first axial compressor stage (Fig. 7) helps us to understand some spectral lines:

- The rotor mode $m = B = 17$, which is cut on since the compressor is transonic, gives $m' = m - 20 = -3$;
- The only propagative interaction mode between the rotor and the stator ($V = 37$ vanes) is $m = B - V = -20$, or $m' = 0$;
- The first interaction mode between the rotor and the 19 inlet guide vanes is $m = B - 19 = -2$.

These few examples emphasize the interest of distinguishing $+m$ and $-m$ if the study is not limited to sound propagation, and if we seek information about noise sources. More details would require a greater number of transducers, but it would be technically very difficult to increase them substantially. Indeed, it would be preposterous to use 88 microphones in order to avoid spatial aliasing up to $|m| = 44$. This is the reason why some tests were performed using a moving microphone just upstream of the engine intake.

III. Spinning Mode Analysis in Front of the Intake Duct Using a Moving Microphone

Basis of the Study

The same data processing as in the previous section can be used with a moving microphone on a rotating ring, and a fixed microphone used as a phase reference (it provides the signal $i = 1$ in Eq. 9). Eq. (9) remains valid, but θ_j is replaced by θ because of the continuous scanning. More precisely, a rotation over 360 degrees lasts about 240 seconds. The cross spectra $S_{12}(f, \theta)$ are sampled every second, which means 240 data in θ . The modes are thus computed up to $|m| = 120$.

This method has been used for many years in the inlet duct of SNECMA turbofan models.⁽¹³⁾ It is difficult to implement inside turboshaft engines because the duct cross section is often non-circular, and also because its size is very small. The idea is to try similar measurements just in front of the inlet, but special care is needed.

Indeed, Eq. (5) reminds us that the in-duct acoustic field has a radial profile function of m and μ . As a result, we see from Eq. (9) that the modal spectrum $|A_m(r)|$ depends on the radius r . In a rigid duct, the sound pressure has a maximum at the wall, and this maximum is often the highest one, since the radial mode μ is generally low. It then suffices in most cases to analyze the modal structure on the duct wall.

Outside the duct, directivity mainly depends on the cut-on ratio:

$$\xi = f_c/f = \sqrt{1 - M^2} \cdot k_T/K \quad (10)$$

i.e. the frequency and the modal structure.^(5,6) For a cut-on wave (radiating in the free field): $0 \leq \xi \leq 1$. Directivity presents only one lateral maximum at frequencies just above f_c (ξ close to 1). The number of lobes increases with frequency (ξ decreasing) and the main maximum becomes more and more axial (but only the mode $m = 0$ radiates on the axis, and directivity reaches its maximum there). A crude estimate of the angle φ_{\max} of maximum directivity is deduced by Rice:⁽¹⁴⁾

$$\sin \varphi_{\max} = \xi \quad (11)$$

It is rather well validated.⁽⁶⁾ As a result, Ref. 15 indicates that modal analysis in the free field requires several scanings at various radiation angles (φ in Fig. 10 below).

Experimental Set-up

The tests were performed on an Arriel engine (Fig. 8) because it can be fitted with an axisymmetric inlet (Fig. 9). This is the simplest configuration for assessing the free-field modal analysis.

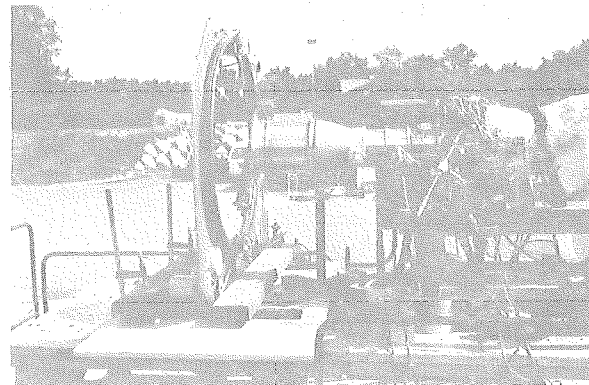


Figure 8 - View of the Arriel turboshaft engine in the Turbomeca test facility, with the microphone rotating ring in front of the inlet.

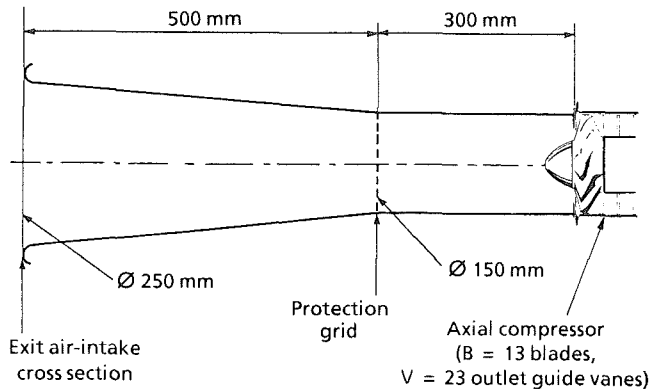
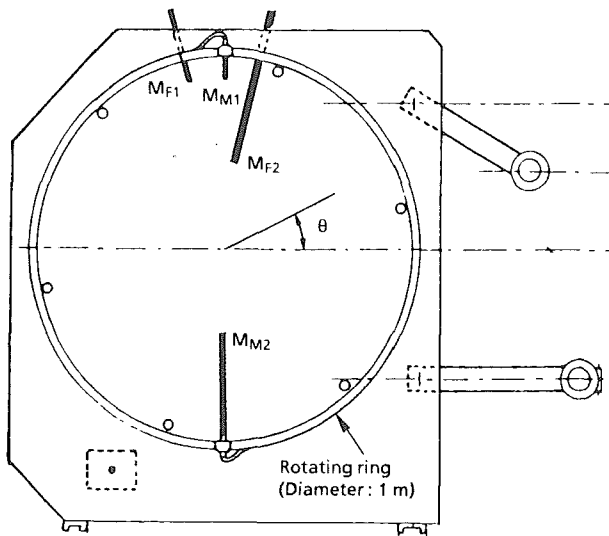
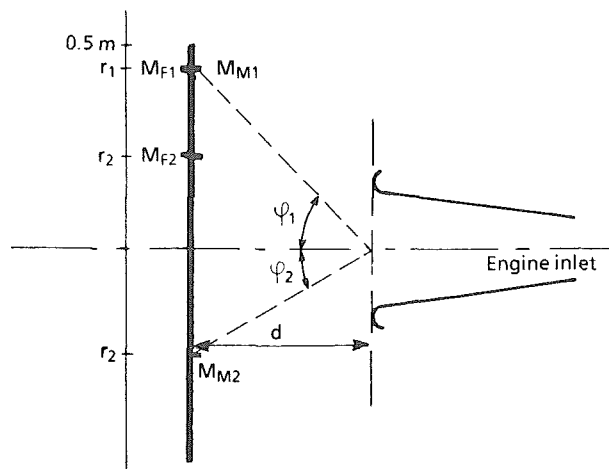


Figure 9 - Diagram of the Arriel air intake for the tests of the previous figure.

Downstream view



Side view



ψ (deg)	d (mm)		
	105	250	370
$r_1 = 445$ mm	77°	61°	50°
$r_2 = 220$ mm	64°	41°	31°

Figure 10 - Free-field spinning-mode measurement with moving microphones.

A rotating ring, 1 m in diameter (Fig. 10), supports two fixed microphones (M_{F1}, M_{F2}) and two moving microphones (M_{M1}, M_{M2}). M_{F1} and M_{M1} are at a radius $r_1 = 445$ mm, M_{F2} and M_{M2} are at $r_2 = 220$ mm. Modal analysis is thus made simultaneously at two radiation angles φ_1 and φ_2 . The distance d between the engine air inlet and the rotating ring can be changed. Six values of φ are scanned in three runs (see the insert in Fig. 10). The distance between the inlet center and the microphones is different for each angle φ . However, no distance correction is attempted since the measurements are made in the very near field of the engine, and the following modal spectra are plotted without any absolute decibel scale.

The signals are digitized by an external clock triggered by a one-per-revolution pulse. Frequency analysis is performed in the range 0 - 20 kHz, in 512 bands (resolution $\Delta f \approx 40$ Hz).

Test Results

The Arriel has two compressor stages, one axial and one centrifugal. The first compressor is the main noise source radiating through the inlet. It has $B = 13$ blades and $V = 23$ outlet guide vanes (Fig. 9). The tests were run at the following rotational speeds:

$$N = 49000; 50300; 51700 \text{ rpm,}$$

which correspond respectively to the blade passing frequency (BPF):

$$f = BN = 10.6; 10.9; 11.2 \text{ kHz.}$$

The rotor is transonic and the rotor-alone mode $m = B = 13$ becomes propagative at $N = 49000$ rpm. A frequency spectrum (Fig. 11) shows that multiple pure tones (harmonics of N) begin to appear, but the BPF strongly dominates in the audio-frequency range. For this reason, only BPF is analyzed in the following results. According to Eqs (10) and (11), $\varphi_{\max} \approx 30$ deg at the three frequencies under study for radiation of $m = 13$ by a duct of diameter 25 cm (φ_{\max} would vary from 84 to 70 deg when the BPF is increased, if it were directly radiated by the compressor duct, of diameter 15 cm, because f_c would be higher in Eq. 10).

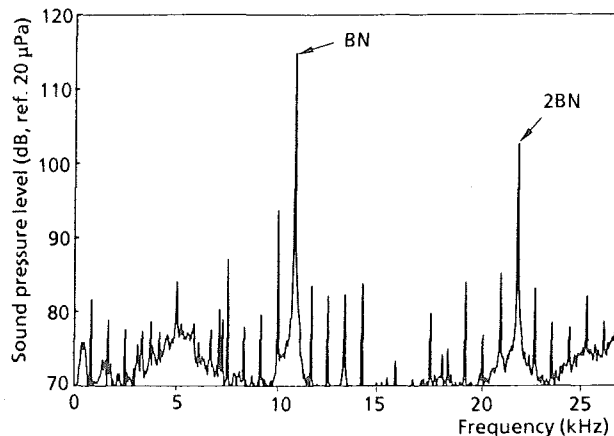


Figure 11 - Upstream near-field acoustic spectrum of the Arriel measured on the rotating ring: $N = 50300$ rpm, $\varphi \approx 60$ deg.

The modal spectra at BPF, $f = 11.2$ kHz, are plotted together in Figure 12 for the six angles φ (the tests at the two lower speeds are not shown, but they lead to similar comments). The two short horizontal lines in the upper left corner of each curve indicate the total tone level in the analyzed bandwidth, L_{tot} , and the coherent level, L_{coh} , i.e. the sum of all the modes. The fact that $L_{\text{coh}} \approx L_{\text{tot}}$ means that the acoustic field remains spatially coherent outside the duct, at the measurement locations. This is a prerequisite for getting consistent results. The mode $m = B = +13$ is the most intense, as expected. It dominates by about 20 dB at $\varphi = 40$ deg and its directivity has a secondary

maximum around 65 deg. The second intense mode is the cut-on mode due to the rotor/stator interaction, $m = B - V = -10$. It radiates at lower angles, $\varphi = 30$ to 40 deg, because ξ in Eq. (11) is smaller (Eq. 11 gives $\varphi_{\max} = 26$ deg for a duct diameter of 25 cm). Some other modes appear in the cut-on range ($-13 \leq m \leq +13$). They are due to interactions between the rotor and long-scale flow distortions.⁽¹⁶⁾ These low-order modes are more clearly seen at $\varphi = 30$ deg, where they lie 10 dB above the background level, because they radiate close to the axis.

Prediction of Free-Field Noise Radiation

The scope of the previous spinning mode analyses was to better understand the noise sources in order to predict the free field directivity. The computation is based on the Tyler and Sofrin model.^(5,6) It extends the classical problem of radiation from a circular piston set in an infinite flange to non-plane waves. The prediction is thus limited to the front quadrant ($0 \leq \varphi \leq 90$ deg). Very briefly, the principle is as follows. Directivity is deduced at a given frequency from the acoustic field in the exit plane of the duct. It is obtained by integrating the contributions of all the point sources in this cross section. The phase shifts between the various point sources are of course the prime parameters. They are related to the space structure of the propagating waves, which explains the emphasis given to the spinning mode reduction.

More details about the calculation method for the present purpose can be found in Ref. 17, along with an application to the Makila turboshaft engine. Because of the lack of information about the actual noise sources in that reference, the radiating modes were deduced from the possible rotor/stator interactions, and from the cut-off properties of the duct (see the previous section). The source intensities are estimated by an assumed decrease in the pressure on the successive blade loading harmonics, as was done first by Lowson.⁽¹⁸⁾

The following computations for the Arriel take into account the modes $m = B = 13$, $|m| = |B - V| = 10$ and a lower interaction mode, say $|m| = 7$ (note that the radiations of $+m$ and $-m$ are identical). The theoretical free-field directivities are plotted in Fig. 13. The sound power level (integral of directivity pattern) is arbitrarily adjusted here to 100 dB for each mode, and the observer's distance is 20 m. The curves confirm the previous comments. For instance, Eq. (11) gives $\varphi_{\max} = 18$ deg for $|m| = 7$, $\varphi_{\max} = 26$ deg for $|m| = 10$, and $\varphi_{\max} = 33$ deg for $|m| = 13$, for a duct diameter of 25 cm and at $f = 11.2$ kHz. These values are close to those of Fig. 13 although the duct is slightly conical (see Fig. 9). It is also assessed that the directivity of $|m| = 13$ has two lobes around 40 deg and 60 deg, as was found in the modal spectra of Fig. 12.

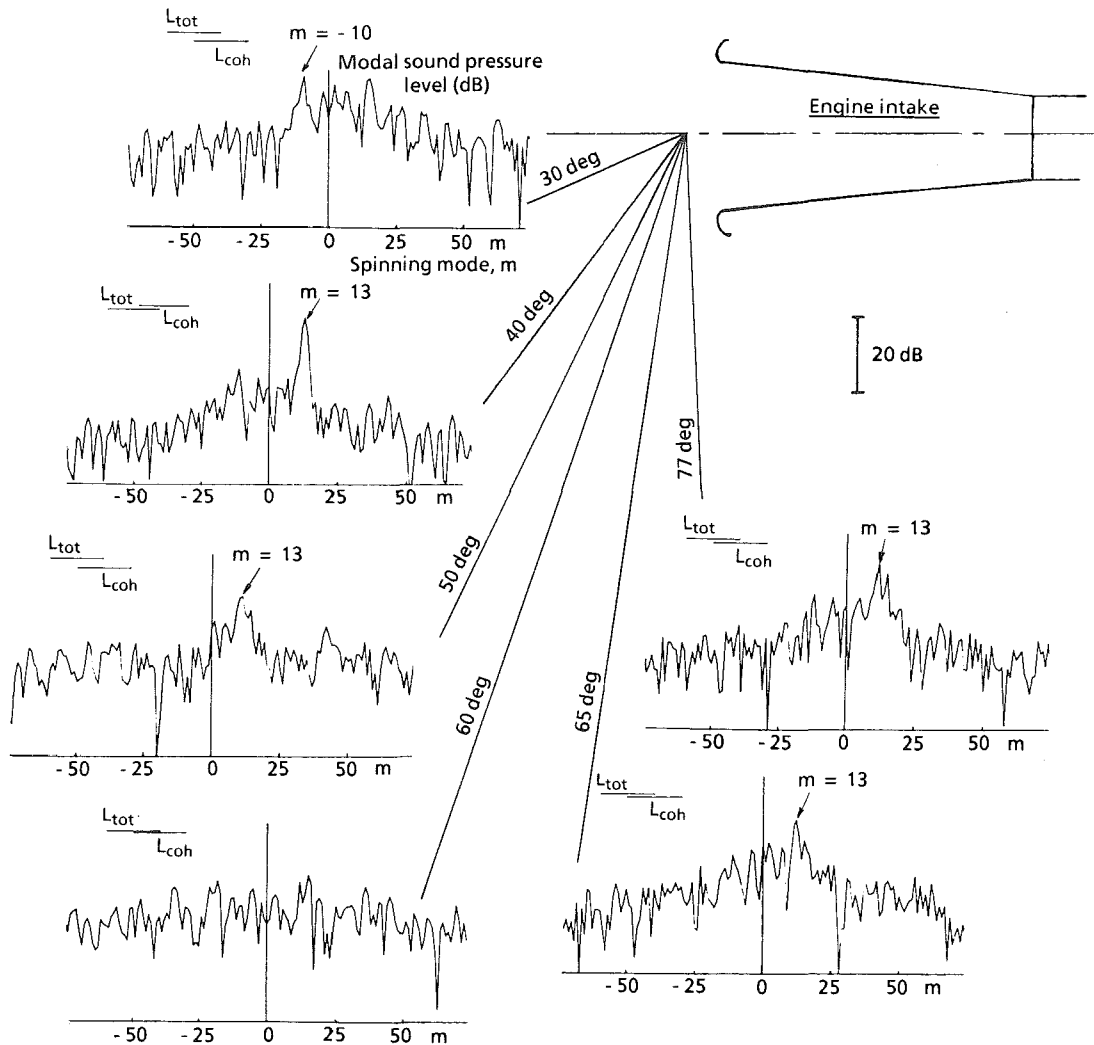


Figure 12 - Spinning-mode spectra of the Arriel at the blade passing frequency for several upstream radiation angles: $N = 51700$ rpm, $f = 11.2$ kHz, bandwidth $\Delta f = 32$ Hz.

The final predictions for the three frequencies under study are compared with the Turbomeca measurements in Fig. 14. The tests were run in the facility shown in Fig. 1, the microphone is 20 m from the engine, and at the same height (3 meters) as the engine centerline. The microphone is moved by a trolley, with automatic stops every 10 degrees. The concrete ground (clear semicircle of radius 30 m in Fig. 1) is considered as a perfect reflector for the acoustic waves, but Ref. 19 reports that a conventional correction of 3 dB at high frequencies may be inaccurate in some directions. Indeed, the oblique radiation of a mode towards the ground is reflected into another direction. This effect explains the level found on the axis ($\varphi = 0$) which could be only due to a plane wave (or more generally a mode $m = 0$) in the case of radiation in an anechoic environment (see the results for modes $m \neq 0$ in Fig. 13). On the contrary, Fig. 12 shows that the mode $m = 0$ is not generated, or if at all, its level is very low. The exact calculation of ground reflections (Ref. 19) is now included in the computer program of Ref. 17.

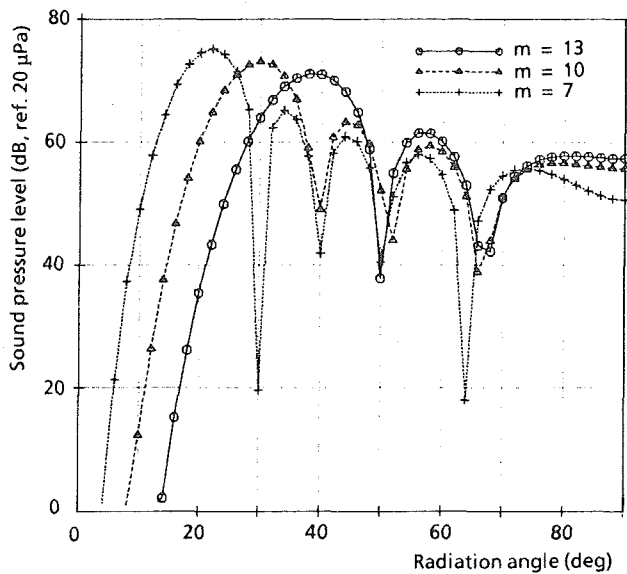


Figure 13 - Computed free-field directivities of spinning modes $|m| = 7, 10$ and 13 radiated by a duct of diameter 25 cm at $f = 11.2$ kHz. Sound power level for each mode: 100 dB, re. 1 pW. Observer's distance to the engine: 20 m.

The predictions in Fig. 14 (and in Fig. 13) are limited in the front arc ($0 \leq \varphi \leq 90$ deg), as previously explained, but we find that the BPF level is much lower in the rearward arc (see for instance Fig. 2). Some differences between computation and experiment do appear near 90 deg, because of the boundary condition on the reflecting flange introduced into the theoretical model. At lower angles, the agreement is rather good although the rotor/flow distortion interaction is crudely modeled by only one mode ($|m| = 7$). The angular location of the maximum is well predicted, and the ground reflections lead to the adequate sound pressure levels around the axis.

IV. Conclusion

There are three possible means for reducing helicopter engine noise:

- ☛ By acting on the sources, which requires a better understanding of the generation mechanisms;
- ☛ With acoustic linings inside the engine intake, whose optimization depends upon the wave incidence angle on the duct wall;
- ☛ By taking advantage of the shape of the intake for modifying the directivity pattern.

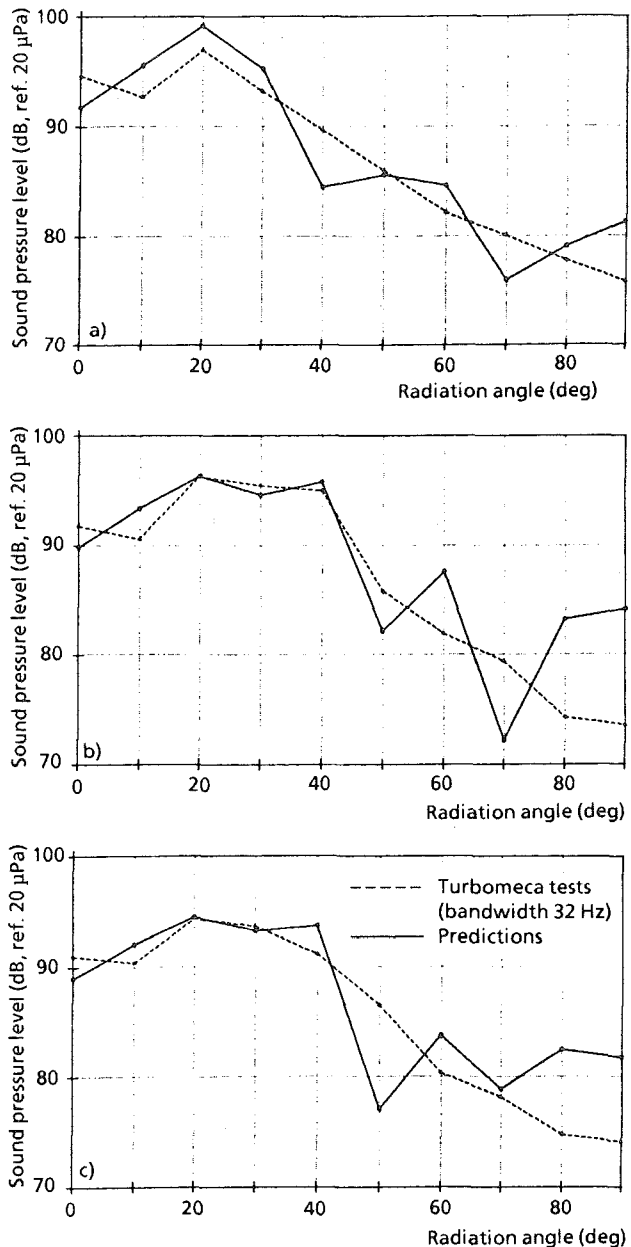


Figure 14 - Predicted and measured far-field upstream directivities radiated by the Arriel at the axial-compressor blade passing frequency. Microphone distance to the engine: 20 m; height above the ground: 3 m.
a) $N = 49000$ rpm, $f = 10.6$ kHz
b) $N = 50300$ rpm, $f = 10.9$ kHz
c) $N = 51700$ rpm, $f = 11.2$ kHz

Accurate knowledge of the spatial (or modal) structure of the sound field propagating in the inlet duct (or in the nozzle) is required in every case. The study is focused on the blade passing frequency generated by the first compressor stage, which dominates the acoustic spectra. Two modal analysis techniques were implemented. The first one uses an array of fixed, flush-mounted microphones on a duct cross section. We found that the spinning mode reduction yields interesting results even if the cross section is not circular. However, due to the small number of transducers, applying this technique at high frequency becomes difficult because many modes may propagate inside the duct, and problems appear as a result of spatial aliasing.

Another method was tested, which uses a moving microphone just outside the engine intake. The acoustic field remains spatially coherent at the measurement locations, thus validating the approach. The detected modes are introduced as input data into a computer code based on the Tyler and Sofrin model to predict free-field directivity. Results are in good agreement with Turbomeca's tests, provided ground reflections are properly taken into account.

Our current research is twofold. Theoretical work consists in extending the radiation computation to more complex duct cross sections. Basic experiments are being performed in an anechoic room with duct elements modeled after the actual engine inlets. In these tests, spinning modes are synthesized by a ring of compression chambers. This work is expected to contribute to the development of downtown heliports, since one of the most challenging problems to be solved is aircraft noise during take-off where engine noise may be predominant (the other acoustic challenge is the main-rotor blade/vortex interaction in descent flight).

Acknowledgments

This work was supported by a contract with Turbomeca. The spinning mode data processing with fixed microphones is due to D. Blacodon. S. Canard-Caruana provided with the data processing applying to a moving microphone. The authors also thank A. Farrando, P. Joubert and B. Claverie, from Turbomeca, for their involvement in the tests and for their experimental results used in the last section.

References

- 1 Damongeot, A., d'Ambra, F., and Masure, B., "Towards a Better Understanding of Helicopter External Noise", Proceedings of the 39th Annual Forum of the American Helicopter Society, St-Louis, May 1983, pp. 445-457.
- 2 Janakiram, R.D., Smith, M.J., and Tadghighi, H., "Importance of Engine as a Source of Helicopter External Noise", AIAA Paper 89-1147, April 1989.
- 3 Farrando, A., "Helicopter Turboshift Engine Acoustic and Infrared Studies and Tests", Paper No. 87, 12th European Rotorcraft Forum, Garmisch-Partenkirchen, Germany, September 1986.
- 4 Guédel, A., and Farrando, A., "Experimental Study of Turboshift Engine Core Noise", Journal of Aircraft, Vol. 23, No. 10, October 1986, pp. 763-767.
- 5 Tyler, J.M., and Sofrin, T.G., "Axial Flow Compressor Noise Studies", Society of Automotive Engineers Transactions, Vol. 70, 1962, pp. 309-332.
- 6 Léwy, S., "Exact and Simplified Computation of Noise Radiation by an Annular duct", Inter-noise Proceedings, Avignon, France, Aug. - Sept. 1988, Vol. 3, pp. 1559-1564.
- 7 Cummings, A., "Sound Transmission in Curved Duct Bends", Journal of Sound and Vibration, Vol. 35, No. 4, 22 August 1974, pp. 451-477.
- 8 Cabelli, A., "The Acoustic Characteristics of Duct Bends", Journal of Sound and Vibration, Vol. 68, No. 3, 8 February 1980, pp. 369-388.
- 9 Rostafinski, W., "Monograph on Propagation of Sound Waves in Curved Ducts", NASA Reference Publication RP-1248, January 1991.
- 10 Joppa, P.D., "Acoustic Mode Measurements in the Inlet Duct of a Turbofan Engine", Journal of Aircraft, Vol. 24, No. 9, September 1987, pp. 587-593.
- 11 Blacodon, D., and Léwy, S., "Space-Structure Determination of the Acoustic Field Generated by a Helicopter Turboshift Engine", AIAA Paper 90-4012, October 1990.
- 12 Blacodon, D., "Acoustic Spinning-Mode Analysis by an Iterative Threshold Method Applied to a Helicopter Turboshift Engine", DGLR/AIAA Paper 92-02-041, 14th Aeroacoustics Conference, May 1992.
- 13 Léwy, S., Canard-Caruana, S., and Julliard, J., "Experimental Study of Noise Sources and Acoustic Propagation in a Turbofan Model", AIAA Paper 90-3950, October 1990.
- 14 Rice, E.J., "Multimodal Far-Field Acoustic Radiation Pattern Using Mode Cutoff Ratio", AIAA Journal, Vol. 16, No. 9, Sept. 1978, pp. 906-911.
- 15 Nakamura, Y., and Isomura, K., "Detection of Fan Acoustic Mode", AIAA Paper 87-2700, October 1987.
- 16 Hanson, D.B., "Spectrum of Rotor Noise Caused by Atmospheric Turbulence", Journal of the Acoustical Society of America, Vol. 56, No. 1, July 1974, pp. 110-126.
- 17 Gounet, H., and Léwy, S., "Directivity of Noise Radiation by the Inlet Duct of a Helicopter Turboshift Engine", 1st French Conference on Acoustics, Lyon, France, April 1990, in Journal de Physique, Vol. 51, No. C2, February 1990, pp. 1201-1204 (in French).
- 18 Lawson, M.V., "Theoretical Analysis of Compressor Noise", Journal of the Acoustical Society of America, Vol. 47, No. 1 (Part 2), January 1970, pp. 371-385.
- 19 Léwy, S., and Gounet, H., "Modification of the Radiated Sound Directivity Due to Ground Reflections: Application to Static Tests of Helicopter Turboshift Engines", Inter-Noise 91 Proceedings, Sydney, Australia, December 1991, Vol. 1, pp. 411-414.